Vulcanization Bonded Natural Rubber-Aluminum by Chemically Modified Graphene Nanoplatelets-Epoxy Adhesive without Primer

Mazatul Nadia Mohd Zafri[1], Noraiham Mohamad[1,*], Mohd Edeerozey Abd Manaf[1], Toibah Abd Rahim[1], Jeefferie Abd Razak[1], Hairul Effendy Ab Maulod[2], Qumrul Ahsan[3], Muhammad Afiq Ani[4], Ming Ming Teng[4]

[1] Fakulti Kejuruteraan Pembuatan, Universiti Teknikal Malaysia Melaka, 76100 Durian Tunggal, Melaka, Malaysia
[2] Fakulti Teknologi Kejuruteraan Mekanikal & Pembuatan, Universiti Teknikal Malaysia Melaka, 76100 Durian Tunggal, Melaka, Malaysia
[3] University of Asia Pacific, 74/A, Green Road, Farmgate, Dhaka-1205, Bangladesh
[4] HML Auto Industries Sdn Bhd, Taman Jati, 45800 Kapar, Selangor, Malaysia

ARTICLE INFO	ABSTRACT
  	Passive engine mounts have been widely used as the simplest solution to isolate the vibration, noise, and harshness from the engine and chassis for a smooth ride. It is mainly made from rubber and metal, requiring rubber-to-metal bonding. Most studies of rubber-to-metal via adhesive bond report the adhesion properties with the help of a primer. In this study, an adhesive system of graphene nanoplatelets (GNPs) reinforced epoxy resin was investigated for their potential to bond the natural rubber composites (NR) with aluminium alloy (AL-alloy) without any application of primer to assess the GNPs' unique contribution to the adhesion criteria. Chemically treated GNPs were mixed into an epoxy system via an ultrasonication method at 0, 0.5, 3.0, and 7.0 wt% loading variation. The epoxy/GNPs (E-GNP) adhesives were then applied to bond pre-etched Al-alloy sheets with NR composites through the vulcanization bonded. The vulcanization was taken placed in a hot press machine under the temperature of 140°C, a pressure of 100 kg/cm^2 for 10 minutes before the samples were subjected to the peel test following ASTM D429. The bonding characteristics were further supported by morphological, compositional, thermal, and structural analyses via Scanning Electron Microscopy, Fourier Transform Infrared Spectroscopy, Differential Scanning Calorimetry, and X-Ray Diffraction. From the results, the E-GNP adhesive system has proven to increase the maximum peel strength of the NR composites-Al alloy by up to 170 % if compared to the control epoxy system. The findings would be a promising technology for improving bonding strength between rubber-metal in diverse applications.

1. Introduction

Nowadays, the automotive industry seeks lightweight components to bring up their new models, greener choices and fuel saving. Hirsch [1] states that lightweight materials can help improve fuel

---

* *Corresponding author.*
E-mail address: noraiham@utem.edu.my

efficiency. The new models would also be equipped with numerous luxury, convenience, performance, and safety accessories, as their customers demand. Therefore, the use of lightweight materials is very crucial. Current industrial demands for lightweight materials are aluminium alloys (Al-alloy). The commonly used joining methods for engine mounting systems are fasteners and adhesives.

According to Heide-Jørgensen *et al.,* [2], rubber and metal bonding can be attained by mechanical fixation or chemical and physical adhesion. The bonding methods between rubber and metal are brass plating, vulcanization, or adhesion through primer and binder. This study applies a chemical approach using thermoset resin adhesive, assisted by a vulcanization bonding process to bond NR-Al alloy. Addressing by Souid *et al.,* [3], the vulcanization bonding process remains poorly understood despite the vast and growing range of rubber-to-metal bonded assemblies used in industrial applications to reduce noise and vibration. This method molds and vulcanizes raw rubber onto a metallic surface coated with an adhesive reactive bonding layer. Hence, it allows the molding of complex shapes with bonded metallic inserts, not as the "post-vulcanization bonding" technique. However, it is complicated as it involves various diffusion phenomena, including chemisorption, bulk, and interfacial crosslinking reactions. Still, the method has proven to be more efficient for rubber-metal bonding since efficient chemisorption and cross-bridging reactions allow the generation of chemical adhesion at the different interfaces.

Mullins *et al.,* [4] have stated that joining by adhesive finds widespread use in various applications such as automotive, aerospace, appliance, and electronics. Higgins [5] and Banea and Silva [6] agree that epoxy-based adhesives find their place in these vital applications due to their excellent mechanical properties. According to Hu *et al.,* [7], epoxy-based thermosets can be identified by high strength, excellent adhesion to numerous metallic and nonmetallic substrates, possess slight shrinkage during and after cure, and high resistance to chemicals and extreme temperatures. Rahmani and Choupani [8] mentioned that epoxy possesses relatively high strength and modulus at room temperature, resulting from its highly crosslinked molecular structure, which is dissimilar from other polymer-based adhesives. Epoxy adhesives have shown many advantages, such as lightweight, high availability of the resin, and low cost. As Poornima *et al.,* [9] reported, epoxy adhesives show ease of processing, including low shrinkage during curing, a wide range of temperatures, low pressure for fabrication, and reasonable control over the degree of crosslinking. Besides, Mullins *et al.,* [4] emphasize that adhesives limit the use of metal fasteners, which are frequently exposed to corrosion. Despite their slow cure speed and high brittleness, epoxy-based adhesives are used because of their hardness and excellent weather resistance characteristics. Pradhan *et al.,* [10] highlighted that the properties of cured epoxy adhesives could be modified using the curing agent and the curing process. In contrast, Poornima *et al.,* [9] state that epoxies' essential brittleness has finite their application in fields requiring high impact and fracture strengths, such as reinforced plastics and matrix resins for composites and coatings. Hence, modifiers could be added to epoxy resins to overcome their limitation.

Various techniques have been developed to overcome the disadvantage of epoxy resins and fulfil these requirements. As Wang *et al.,* [11] highlighted, enhancing the toughness, mechanical and thermal properties of epoxy resins by reinforcing the inorganic nanofillers has attracted considerable scientific and industrial interest. Numerous efforts have been made to enhance and increase epoxy adhesion strength, wear performance, chemical stability, electrical insulation, etc., by reinforcing the resins with nano-fillers. Among the nanofillers are carbon nanotubes (CNT), nano-silica, hybrid nano-alumina and nano-silicon carbide, hybrid carbon fiber (CF)-nanodiamonds, CF-multi-walled-CNT, CF-organo-modified montmorillonite with varying degrees of success [12-17]. Since the emergence of carbon nanotube research in the mid-1996s, carbon-based nanomaterials have gained interest

among researchers and industrialists to enhance diverse properties for various systems [18]. Recently, the appeal falls on the graphene nanomaterial, a single-atom-thick sheet of sp^2-bonded carbon atoms with high specific area, mechanical, electrical, thermal, and chemical stability properties [19]. With an estimated Youngs modulus of 1 TPa and ultimate strength of 130 GPa, graphene is labelled the most robust material ever. Graphene platelets are electrically conductive at 6000 S/cm and thermally conductive at 5×10^3 W/mK at room temperature [20]. According to Smith *et al.,* [19], the platelets' large specific surface area is up to 2630 m^2/g due to the platelets consisting of very fine graphene of 0.34 nm in thickness and ~1 μm in the lateral dimension.

Quan *et al.,* [21] state that graphene's effects on epoxy's mechanical properties, electrical conductivity, and fracture toughness have been widely studied. Based on the studies, it is reported that the addition of 0.2 wt.% graphene oxide into the neat epoxy increased Young's modulus from 2.93 GPa to approximately 3.1 GPa, with the fracture toughness increase from 0.49 MPam$^{1/2}$ to 0.75MPam$^{1/2}$. The primary toughening mechanism recognized is the debonding and crack bridging of the graphene oxide platelets. Meanwhile, Rafiee *et al.,* [22] studied graphene-modified epoxy nanocomposites' fracture and fatigue performance. They found that adding 0.125 wt.% of functionalized graphene sheets has improved the neat epoxy's fracture toughness by 65 % and the fracture energy by 115 %. In a study by Ahmadi-Moghadam *et al.,* [23], a mutual improvement in Young's modulus and tensile strength was observed with only a small loading of graphene nanoplatelets. Together, they increased the fracture toughness of epoxy by 82 %. In their study, crack bridging is identified as the primary toughening mechanism. Quan *et al.,* [21] concluded that the nanomaterial's excellent damping properties are attributed to the well-dispersed graphene nanoplatelets. It is observed by Mohamad *et al.,* [24] when good vibration and thermal transfer between metal to rubber parts are dispersion-related. They emphasized that these properties are vital in improving engine mounts' efficiency and service. Quan *et al.,* [25] agreed that the application of rubber nano-modified structural epoxy adhesive had expanded extensively in various industries, including automotive and aerospace. It is the effect of the high fracture energy and good resistance to fracture of the modified adhesives.

Mohamad *et al.,* [26] have stated that all types of rubbers and the polymeric system will undergo thermal degradation reactions, leading to a loss of mechanical properties at elevated temperatures. Hence, the graphene nanoplatelets are hypothesized as an alternative filler material to enhance epoxy composites' degradation resistance to a higher temperature and improve adhesion strength. Therefore, this research discusses the feasibility of incorporating chemically modified graphene nanoplatelets in epoxy resin. This research investigates the feasibility of enhancing bonding strength between NR composites with Al-alloy using an epoxy adhesive system by varying GNPs loading via a vulcanization bonding process without a primer. The GNPs loadings of 0, 0.5, 3.0, and 7.0 wt% in the epoxy adhesives to bond the NR composites-Al alloy were investigated. The epoxy/GNPs (E-GNP) adhesives were prepared via ultrasonication mixing. The NR and Al-alloy sheets were bonded together using a hot press machine at constant parameters and subjected to peel tests using the UTM machine per ASTM D429. Further investigations were carried out using Scanning Electron Microscopy (SEM), Fourier Transform Infrared Spectroscopy (FTIR), Different Scanning Calorimetry (DSC), and X-Ray Diffraction (XRD).

2. Methodology
2.1 Materials

Graphene Nanoplatelets (GNPs) KNG-50 was supplied by Xiamen Graphene Technology Co. Ltd, China. The amounts used in this study were 0, 0.5, 3.0, and 7.0 wt%. The utilized adhesive base was

thermoset epoxy resin, CP 360 Part A with hardener, CP 360 Part B supplied by Terra Techno Engineering (Malaysia) Sdn. with ultimate pot life, cure and hardening times were three, seven, and 24 hours at 25°C, respectively. Ethanol supplied by SystermChemAR was used as the organic medium for the dispersion of graphene nanoplatelets. The aluminium 6061-T6 was used with a 1.5 ± 0.05 mm thickness. The aluminium sheet was cut into the desired shape using a laser cutting machine. Meanwhile, the NR60 compound was supplied by HML Auto Industries Sdn Bhd.

2.2 Preparation of Chemically Modified Graphene Nanoplatelets-Epoxy Adhesive

Before the adhesive synthesis, a specific range of GNPs to epoxy ratio was calculated and weighed for control sample without filler (0 wt% GNPs) and samples with fillers (0.5, 3.0, and 7.0 wt% GNPs). The GNPs have then undergone a chemical modification in the ethanol. It follows with sonication in a bath sonicator for 3 hours. Then, the mixture was removed from the ultrasonic bath onto a hotplate. After that, the liquid epoxy resin was added to the mixture. The mixing was thoroughly assisted by manual stirring carried out for 30 minutes. All the related procedure in preparing the E-GNP adhesives is simplified as in Figure 1.
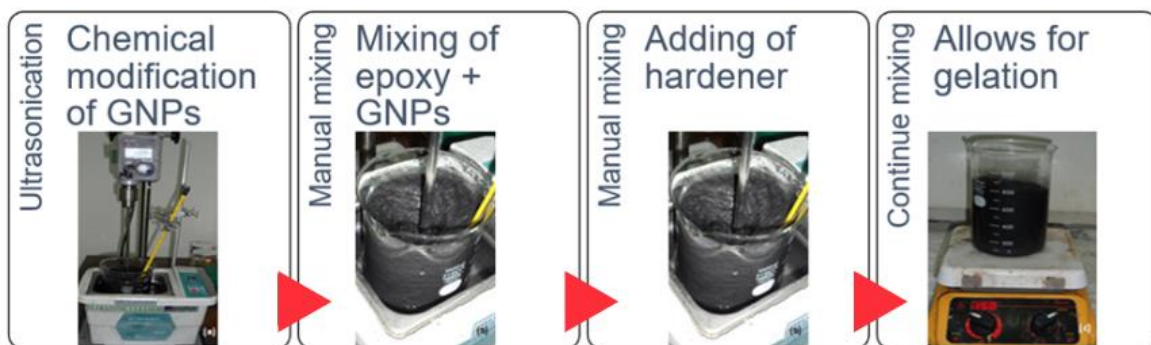

Fig. 1. The preparation process of E-GNP adhesive matrix using a sonicator in ultrasonic bath and hotplate

The mixture was added with the hardener CP360B at the ratio of 2: 1 weight fraction epoxy/hardener and was mixed manually for 3 minutes to obtain the final E-GNP adhesive. The modified adhesive was removed from the hotplate once it reached the gelation stage. The process was repeated for the sample without GNPs filler (0 wt% GNPs). The overall formulation is summarized in Table 1.

Table 1
Formulation of GNPs modified adhesive

Ingredients	% /Volume /Ratio			
	E-GNP0	E-GNP0.5	E-GNP3	E-GNP7
GNPS	0%	0.5%	3.0%	7.0%
Ethanol	100 ml	100 ml	100 ml	100 ml
Epoxy: Hardener	2: 1	2: 1	2: 1	2: 1

2.3 Preparation of Aluminium Alloy Surface

Al-alloy went through the sandblasting process. The samples were submerged in ethanol for 5 minutes and acetone for 5 minutes. The samples were then rinsed under the distilled water before being immersed in the alkaline solution for 3 minutes. The sample preparation was conducted in the

ultrasonic bath. The alkaline solution (NaOH) comprised 5% alkaline and 95% distilled water with a pH of 10. The pH value of the alkaline solution was indicated by using litmus paper. The samples were dried in the oven at 70°C for 45 minutes. Each sample was kept in a box containing silica gels and placed in a drying cabinet before use.

2.4 Vulcanization Curing by Hot Press

The vulcanization of NR and E-GNP adhesive was conducted to form NR composites-Al alloy bonding system before the peel test in a hot press machine. The mold cavity of 6.3 mm x 125 mm x 25 mm for thickness, length, and width was designed according to ASTM D429 (Method B) standards. It was properly cleaned to avoid any contamination during the vulcanization process. In this step, the amount of NR composite compound was first measured based on the mold cavity volume.

Then, the pre-applied E-GNP0, E-GNP0.5, E-GNP3 and E-GNP7 adhesives on Al-alloy plates (Figure 2) were first placed into the mold cavity followed by the uncured NR composite compound (refer to Figure 3). The samples were preheated in a hot press machine for 3 minutes. The vulcanization process took place at 140°C, a pressure of 100 kg/cm^2 for 10 minutes. Then, the samples were cooled down for 3 minutes. Before undergoing a peel test, the vulcanized samples were kept in a box containing silica gel and placed in a drying cabinet for 24 hours.
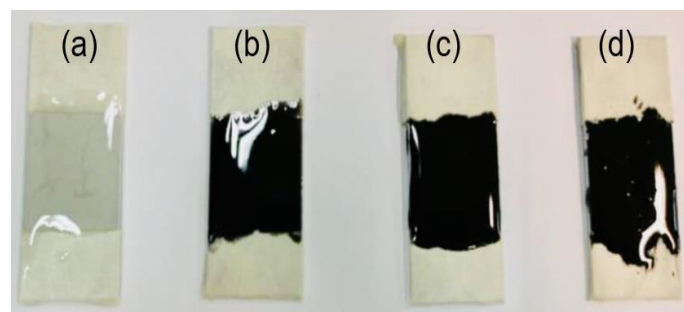

Fig. 2. Adhesives on Al-alloy sheets for (a) E-GNP0, (b) E-GNP0.5, (c) E-GNP3 and (d) E-GNP7
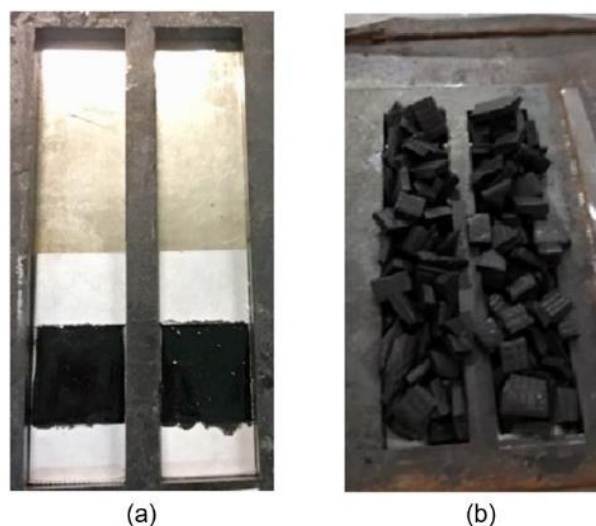

Fig. 3. In preparation for vulcanization bonding, (a) Al-alloy sheets with adhesives are placed in the mold cavity, and (b) the unvulcanized rubber compounds are added on top of the sheets

2.5 Peel Test

Using Method B of ASTM D429, the adhesive-bonded rubber-metal was peeled at a 90-degree peel strip test. The bonded area was 25 mm times 25 mm in the middle of the metal piece with a thickness of 20±2 μm using a paintbrush. The testing was carried out using a Universal Testing Machine (Shimadzu AGS-X Series) at room temperature at a cross-head speed of 50 mm/min, as shown in Figure 4 to measure the maximum peel force, F. The flat peel test fixture was fabricated according to the design in Figure 5.

Fig. 4. The 90 degrees peel test performed on the rubber-metal bonding

Fig. 5. The peel test samples

The nominal peeling energy was calculated from the measured F value. The energy released for nominal peeling energy, T, for an interface crack propagation, was calculated using Eq. (1).

$$T = F\,(\lambda - \cos 0)w - Wh \tag{1}$$

where λ is the extension ratio of the peel leg (λ = 1 + e, where e is the minimum strain in the peel leg), 0 is the angle of the peel, W is the strain energy density in the leg, w is the width of the rubber and h is the thickness of the rubber when it was in an unstrained state. When the extension in the peel leg is ignored, both λ and W are taken as λ =1 and W = 0. Since the peeling was carried out at 90°, the equation's simplified version is stated in Eq. (2).

$$T = F/w \tag{2}$$

2.6 Analyses Methods

X-ray diffraction (XRD) measurements were performed using a PANalytical X'Pert Pro diffractometer, and the data was analyzed using X'Pert PRO software. The used X-ray source was CuKα radiation, and all samples were characterized at the 2θ scanning range of 5° to 90°. The adhesion mechanism of adhesives bonded NR composites- Al-alloy surfaces were analyzed using images captured by a digital camera and Scanning Electron Microscopy (SEM). The magnifications used for SEM observations were from 50X and 500X. Before the examination, the peeled-off surfaces were placed onto aluminium stubs and coated with gold through a sputter coater.

Differential scanning calorimetry measurements were performed using a Perkin–Elmer DSC-7 (United States) analyzer. The sample weights of about 5–10 mg was scanned from -40°C to 300°C under a nitrogen atmosphere at a scan rate of 10°C/min. The samples' glass transition temperature (Tg) and melting temperature (Tm) were determined from the DSC thermogram. The cured adhesive samples with different GNPs loading (0.5 %wt, 3.0 %wt, 7.0 %wt) were tested using the DSC as per ASTM E1356, the standard test method for glass transition temperatures.

The IR spectra were measured with the JASCO FTIR-6100 model for the 450 to 4000 cm^{-1} wavenumbers at a resolution of 4 cm^{-1}. Different functional groups and structural features in the molecules absorb energy at characteristic frequencies. The absorption frequency and intensity indicate the molecule's bond strength and structural geometry.

3. Results
3.1 X-Ray Diffraction (XRD) Analysis of Epoxy/GNPs (E-GNP) Adhesive

Figure 6 shows the XRD pattern for both E-GNP adhesives and pure GNPs. In Figure 6(b), a diffraction peak at ~ 2θ = 24.06° represents the partially crystalline nature of GNPs. The slightly broader peak observed might be due to the combination of graphite and graphene in the commercial GNPs. The GNPs platelets tend to agglomerate and stack into graphite once exposed to the ambient condition.

Meanwhile, the XRD patterns of adhesives in Figure 6(a) show identical characteristics with similar diffraction peaks. There are presences of broader peaks at 2θ = 20.1° in both E-GNP0 and E-GNP adhesives, which were less than the pure GNPs. The intercalation mechanism between epoxy and GNPs resulted in identical 2θ values having similar interspacing with the pure epoxy, E-GNP0. These similar broader diffraction peaks reflect their highly amorphous structure; hence, the GNPs were uniformly dispersed in the epoxy adhesive. The observed broad peak is similar to the one reported by Wei *et al.,* [27].
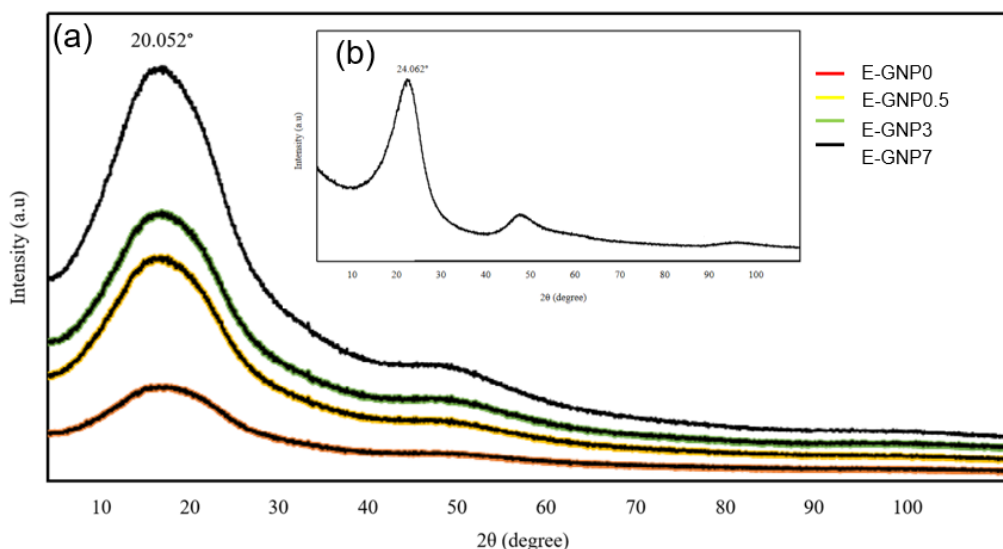
Fig. 6. XRD patterns of (a) E-GNP adhesives and (b) pure GNPs

The intensity of the peak increases corresponds to GNP content's increase, manifesting the increment of crystallinity level but at a different interspacing than graphite oxide. Due to the good dispersion of GNPs, there is no corresponding peak of graphite oxide in the E-GNP adhesive. The summary of the XRD result is tabulated in Table 2.

Table 2
Summary of XRD results of pure GNPs and the adhesives with GNPs

Pure GNPs	Pure Epoxy and Epoxy adhesives with GNPs
$2\theta = 24.06°$	$2\theta = 20.052°$

3.2 Fourier Transform Infrared (FTIR) Analysis of E-GNP Adhesive

FTIR measures the absorption of infrared radiation by sample material concerning the wavelength of the radiation. Using absorption data, one may identify molecular components and structures. FTIR analysis helps identify the functional groups for E-GNP adhesives compared with the control sample. Figure 7 shows IR spectra of cured E-GNP adhesive at different weight percentages and the control sample (cured epoxy adhesive without GNPs).
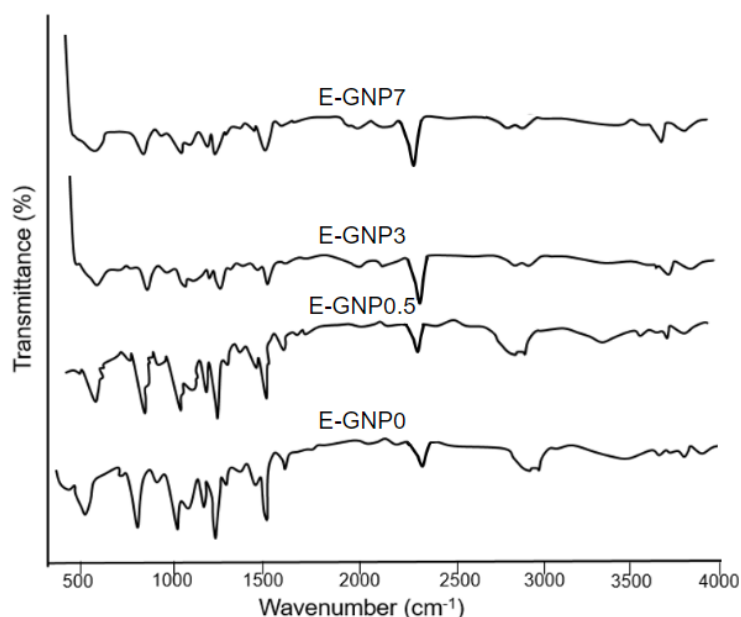
Fig. 7. FTIR spectra of adhesives

From the obtained IR spectra, the dominant peaks of epoxy adhesives with or without GNPs were observed at 2800 to 2900 cm^{-1}, corresponding to the –CH$_2$ and –CH$_3$ stretching modes of the aromatic and aliphatic chains [28]. Meanwhile, around 1100 to 1130 cm^{-1}, the band corresponds to C-O-C and C-O stretching attributed to ether linkages [28]. The IR pattern on the E-GNP adhesives exhibited only slight differences in the intensity at several peaks rather than the formation of new peaks.

Figure 7 shows that the IR spectra of E-GNP adhesives remained nearly constant despite an increase in the weight percentage of GNPs. This observation can be attributed to the role of GNPs as nanofillers, which interact with the epoxy matrix primarily on a physical level rather than a chemical one.

Still, the GNPs in the E-GNP adhesive retained the hydroxyl groups, which later interacted with OH or unsaturated O on the epoxy chains. Characteristic peaks at 2361 cm^{-1} can be attributed to the O−H stretch from strongly hydrogen-bonded –COOH on the GNPs surface. This observation agrees with the study by Atieh *et al.,* [29] for FTIR analysis on carbon nanotube surfaces modified by COOH. The peaks manifest strongly in the E-GNP3 and E-GNP7. GNPs used for the E-GNP adhesive were initially treated with ethanol before mixing. Besides, it normally inherently experienced previous acid treatment during production, providing reactive sites like hydroxyl and carboxylic groups at the plane's basal and edges. On the other hand, Du and Cheng [30] stated that these functional groups in the GNPs were beneficial in indicating the interaction between the GNPs and polymers.

3.3 Differential Scanning Calorimetry (DSC) of E-GNP Adhesive

The compatibility of a thermoset adhesive can be determined by differential scanning calorimetry analysis (DSC), which measures the glass transition temperature (T$_g$) and melting temperature (T$_m$) of a material. DSC analysis also helped study thermal behaviour stability for E-GNP adhesive after curing. DSC examined the thermal characteristics of E-GNP and epoxy adhesives at temperatures ranging from -40 to 300(C with a heating rate of 10(C/min, allowing the identification of glass transition temperatures, Tg, and the melting temperature, T$_m$.

Figure 8 illustrates the scan traces of the DSC thermogram. Referring to the DSC curves, only slight changes were observed in the identification peaks of Tg. It appeared due to the formation of the 3D

network structure of the epoxy matrix chains. It can be concluded that the system achieved a stable form, which restrained them from changing their state under any thermal condition.
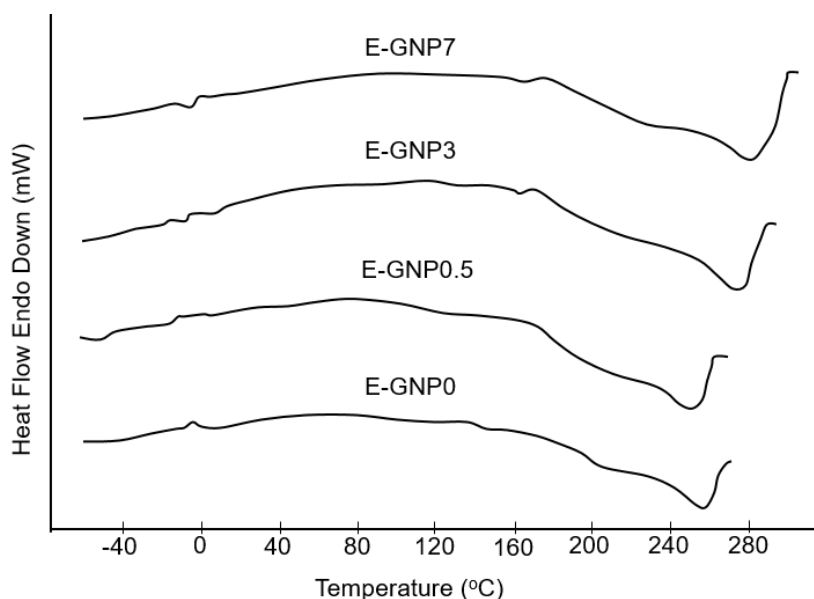

Fig. 8. DCS curves of adhesives

Meanwhile, as depicted in Figure 8, the shift in melting temperature to higher temperature once added with GNPs showed the sample experienced an improved thermal resistance. This is because the thermally conductive GNPs act as the channel for heat dissipation, which helps delay the adhesive system's melting point. However, the curve shows deterioration for E-GNP7 due to agglomeration when GNPs particles were clustering and turning into larger particles [31]. The agglomeration of the GNP in epoxy matrix will disturb the heat transfer path of the adhesive system. This mechanism is illustrated in Figure 9.

The illustration in Figure 9 represents the effect of agglomeration on heat transfer mechanisms. A good dispersion of GNPs gave a shorter distance for the phonon transfer between each particle. It improves the tendency to form interconnected GNPs networks in the matrix, as reported by Kim *et al.,* [32]. However, for the graphene agglomerates, the distances between each agglomerate are far apart, prone to forming a segregated network [32]. This phenomenon caused a longer path for heat transfer. Shorter heat transfer gave a higher melting temperature as the heat did not localize and could be easily transferred out of the body. It was different for the graphene agglomerates as the heat transfer was very slow, which caused the localized heat at a certain point in the body. Based on the melting temperature obtained, it shows that GNP helped increase the adhesive system's melting temperature. Therefore, incorporating GNP at optimum loading allows the existing adhesive system to be utilized at a higher service temperature.
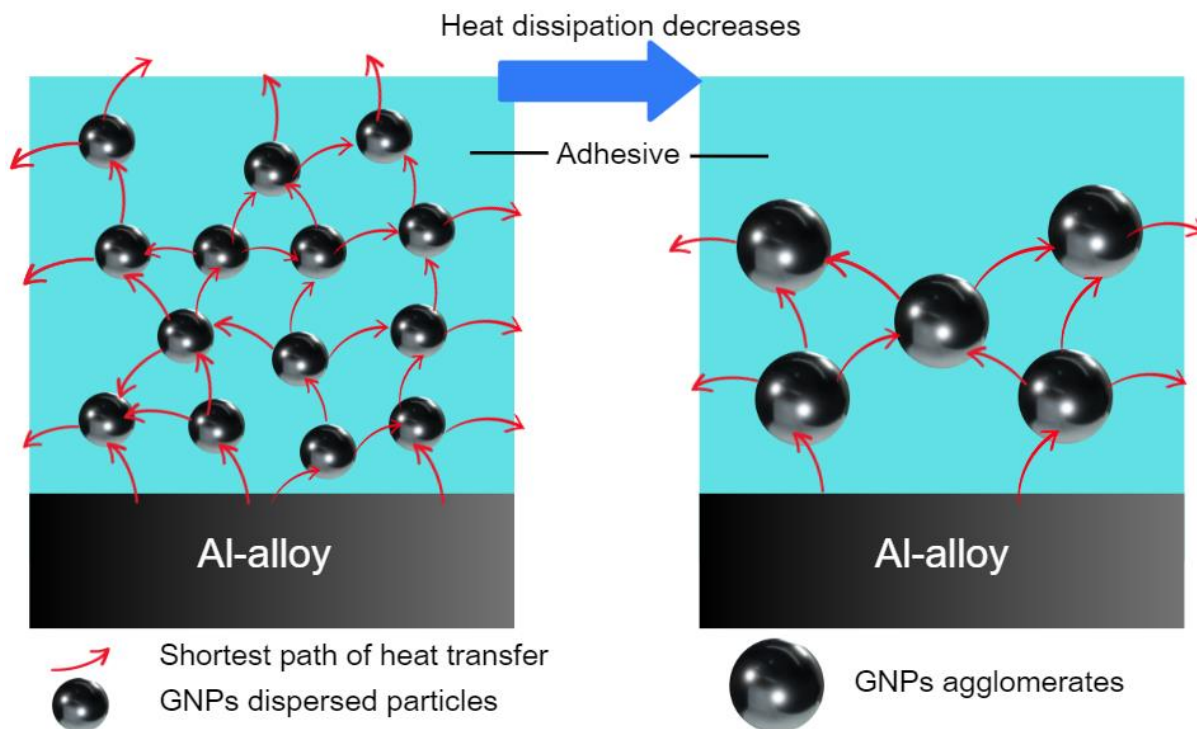
Fig. 9. Illustrations of heat pathways for the effect of GNPs dispersion level

3.4 Peel Strength of NR Composite-Al Alloy
3.4.1 Maximum peel force

The peel test was conducted on control E-GNP0 and E-GNP adhesive samples to determine the effect of GNPs loading on the NR composite-Al-alloy system's bonding strength aided by the E-GNP adhesive. Figure 10 and data tabulated in Table 3 show that E-GNP3 has a higher maximum peel force than the utilized epoxy-hardener system, E-GNP0, representing the control sample in this study. A notable increase was observed with the slight incorporation of GNPs at 3.0 wt% into the system. The maximum peel force for E-GNP3 increased by ~170% from the controlled sample (epoxy adhesive), which showed the maximum peel force at an average of 43.93 N. From the obtained data, it can be concluded that utilizing GNPs in the epoxy adhesive matrix will help increase the maximum force needed to separate the bonding between NR and Al-alloy. However, at 7.0 wt% of GNPs, the maximum peel force reduced drastically to an average of 29.61 N. This reflects the weak bonding strength of the E-GNP7 due to the agglomeration of GNPs filler. The agglomeration issue significantly impacts the properties of E-GNP adhesives. As a result, it becomes evident that the optimal GNPs loading range falls between 3.0 to 7.0 wt% in the E-GNP adhesive system. Incorporating GNPs into the epoxy adhesive matrix at an optimum level enhances the maximum force required to rupture the bond between NR composites and Al-alloy.

Table 3
Comparisons of maximum peel force between adhesives

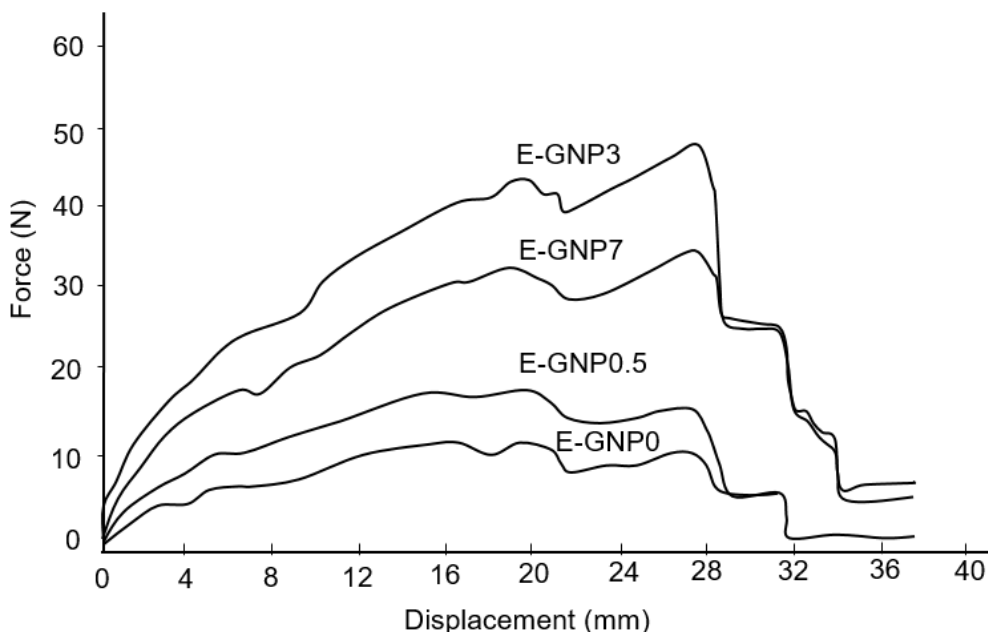| GNP weight percentage (wt%)	Maximum Peel Force (N)	Standard deviation
0 (Epoxy adhesive)	15.95	3.4229
0.5	24.44	1.9869
3.0	43.30	0.7697
7.0	29.61	0.0503

Fig. 10. Maximum Peel Force of different adhesives

3.4.2 Nominal peel energy

The results tabulated in Table 4 show the effect of adding GNPs into the epoxy-hardener system on the nominal peel energy, representing the peel strength of the rubber-metal interface. The nominal peel energy of the E-GNP3 system increased up to ~110 % if compared to the control sample (E-GNP0 adhesive). Hence, modifying an adhesive system using GNP has enhanced the rubber-metal joining system's bonding strength. This is due to the good interaction between the GNP and epoxy matrix, evident from the XRD analyses.

Table 4
Nominal force energy of different adhesives

GNP weight percentage (wt%)	Nominal peel energy (J/m^2)
0 (epoxy adhesive)	823.68
0.5	1064.16
3.0	1760.23
7.0	1187.01

3.5 Morphological Characteristics of NR Composites-Al Alloy Surfaces
3.5.1 Failure mode analysis of peel-off NR composites-Al alloy surfaces

Visual failure analyses were conducted to identify the failure mode of the NR composites-Al alloy surfaces bonded using the epoxy systems, whether through cohesion or adhesive failure. Figure 11 shows the camera images of the peeled-off surfaces of both NR composites and Al-alloy. The visual inspection shows that the E-GNP0 and E-GNP0.5 represent the failure tendency towards adhesion mode with apparently shining smooth surfaces. Meanwhile, the E-GNP3 and E-GNP7 represent higher cohesion mode failure. It is observed from the partially matt with rougher surfaces. These observations were evidence of the higher bonding strength formed by the E-GNP3 than the control E-GNP0 and other adhesives. Adding GNPs into an epoxy adhesive system helps increase the cohesiveness of the adhesive to bond rubber-metal.
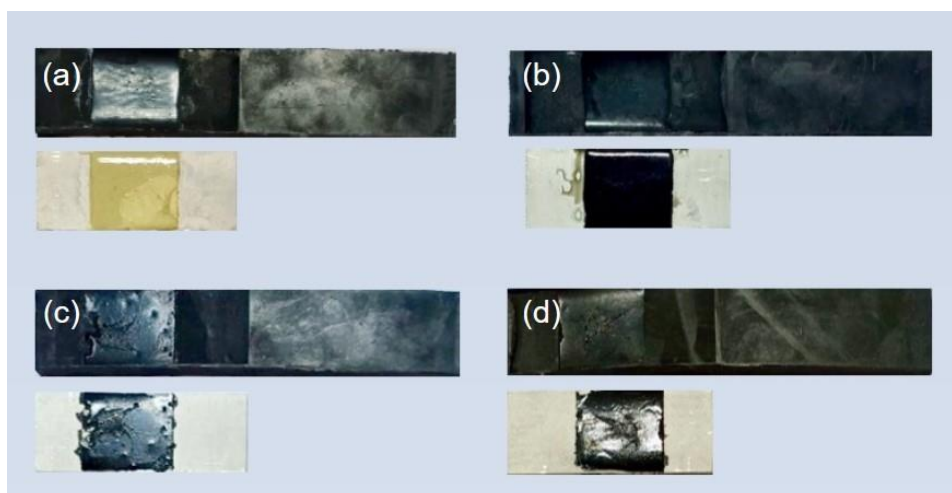
Fig. 11. Failure surfaces of (a) E-GNP0, (b) E-GNP0.5, (c) E-GNP3 and (d) E-GNP7 adhesives

3.5.2 Scanning electron microscopy (SEM) analysis of peel-off NR composite-Al alloy surfaces

Figure 12, Figure 13, and Figure 14 illustrate the SEM micrograph from the peel test fractured surface from both NR composites and Al-alloy surfaces. For epoxy adhesive, NR composites and Al-alloy's fracture surface show smoother surfaces than epoxy filled with GNPs adhesives. The higher the bonding strength, the rougher the fracture surfaces. Besides, the bonding strength between the adhesive and substrate was also influenced by the wettability of the adhesive. Wettability is the tendency of one fluid to spread on or adhere to a solid surface in the presence of other immiscible fluids. It refers to the interaction between fluid and solid phases. Higher wettability indicates a smaller contact angle with the substrate, providing better adhesion and vice versa.

The surface of E-GNP3 adhesive has higher density formation of coalescing dimple-shaped cavities identified as having better wettability, as shown in Figure 14(c). The higher the wettability, the better adhesive dispersion into the substrate. The diffusion of NR particles into E-GNP adhesive particles helps to increase the bonding strength between NR composites-Al alloy. This finding also aligned with the maximum peel force and nominal peel energy obtained. The fracture surface of epoxy adhesive E-GNP0 in Figure 11(a) shows no evidence of NR traces settled on the adhesive's surface on top of the Al-alloy. Yet, the low-density formations of microscale spherical droplets of NR were observed on the adhesive layer in SEM micrographs, as depicted in Figure 12(c). However, there were apparent traces of rubber particles on the fracture surfaces of E-GNP adhesives, especially for E-GNP3 and E-GNP7 (refer to Figure 11(c) and Figure 11(d)), which showed that the fracture occurred due to the failure of the adhesive-rubber interface. It is explained by the traces of rubber (manifested as voids from the peel-off mechanism) distributed along with the epoxy adhesive distribution on the Al-alloy surfaces (Figure 13 and Figure 14).

Figure 15 illustrates the NR composites- Al alloy system's fracture mechanism for epoxy adhesive and E-GNP adhesives. For the NR composites-Al alloy bonded by epoxy adhesive, the spherical-like rubber droplets remain on top of the adhesive layer, showing a high possibility that the fracture occurred due to adhesive failure. Meanwhile, for the one bonded by the E-GNP adhesives, the rubber droplets in the adhesive showed the fracture could have occurred due to the cohesive failure. This situation proves that the strength of E-GNP adhesives is higher than that of E-GNP0. The E-GNP adhesives bonded to a higher density of irregularly shaped coalesce rubber droplets resulting from clustering NR particles, with sizes ranging from approximately 10 to 30 μm. Eakvanich *et al.,* [33]

noted that the individual NR particles typically have diameters of 0.02 to 3.0 µm. This observation suggests an enhanced vulcanization bonding efficacy within the system.
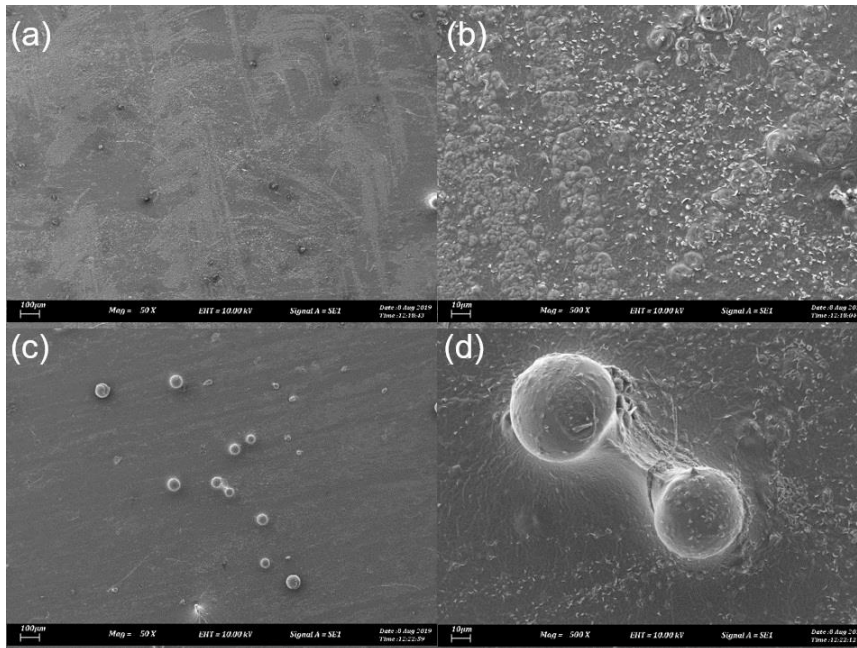

Fig. 12. SEM micrographs of E-GNP0 adhesive on (a-b) NR (c-d) Al-alloy surfaces at different magnifications of 50X and 500X
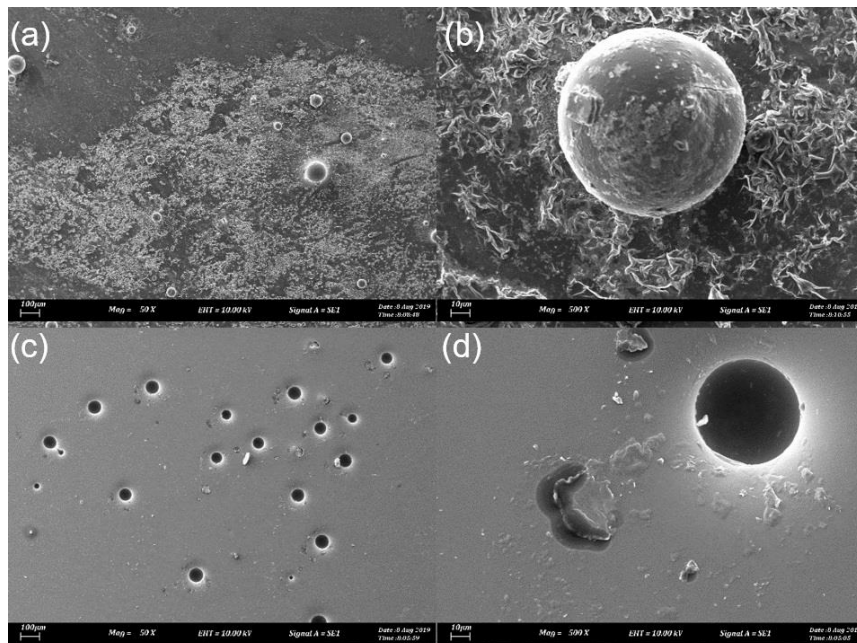

Fig. 13. SEM micrograph of E-GNP0.5 adhesive on (a-b) NR (b-d) Al-alloy surfaces at different magnifications of 50X and 500X
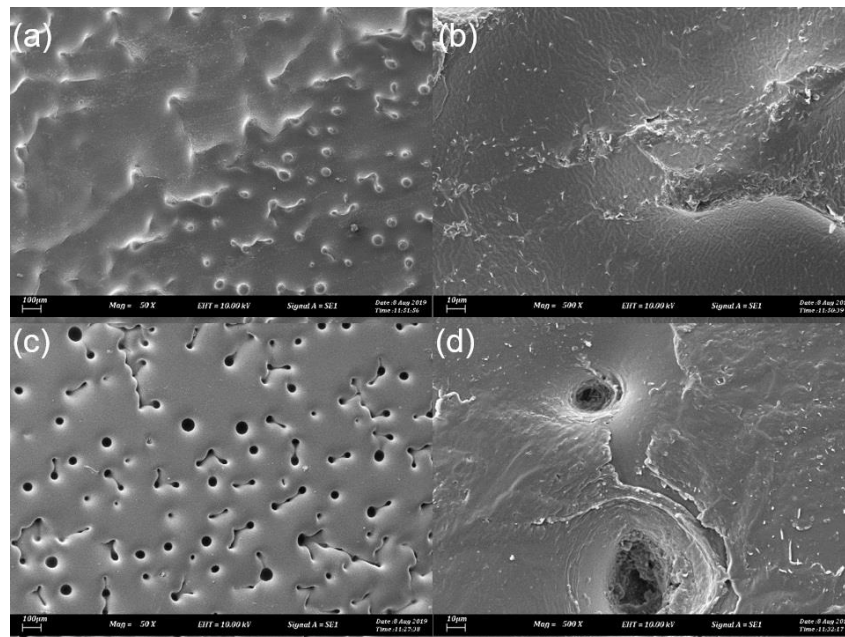
Fig. 14. SEM micrographs of E-GNP3 adhesive on (a-b) NR (b-d) Al-alloy surfaces at different magnifications of 50X and 500X
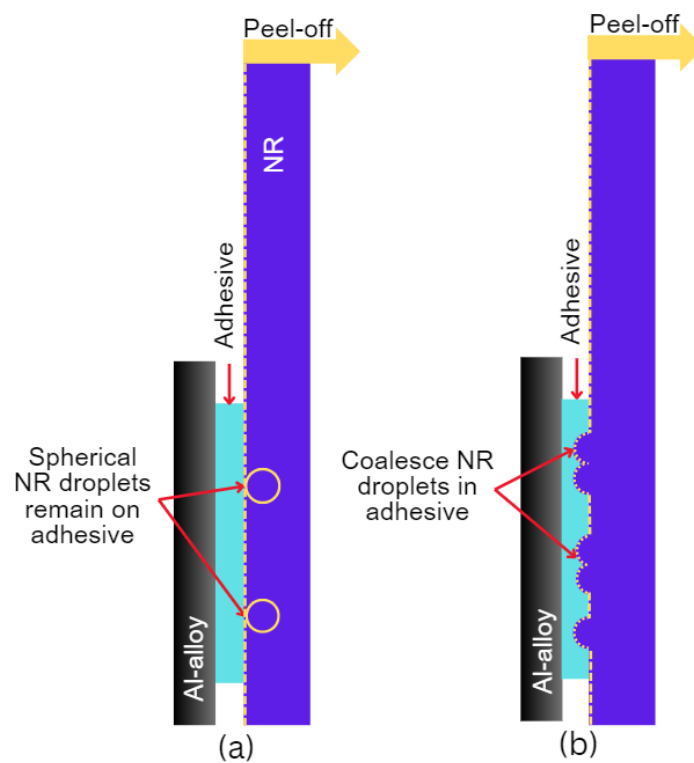

Fig. 15. Fracture mechanism of NR composites- Al alloy system for (a) epoxy and (b) epoxy reinforced with GNPs adhesives

4. Conclusions

Epoxy adhesives filled with different loadings of graphene nanoplatelets (GNPs) have been successfully prepared via chemical modification and vulcanization bonding. Adding GNPs into epoxy adhesive increased the NR composites- Al alloy system's bonding strength if compared to the one

bonded with pure epoxy adhesive. The adhesion strength recorded for epoxy reinforced with GNPs has over 150% of the maximum peel force compared to the control sample. The results are supported by compositional, thermal, morphological and structural characterization by FTIR, DSC, SEM, and XRD. However, the observed increment of maximum peel force to 43 N is still insufficient for the mounting system due to its service requirements exposed to dynamic stresses and high service temperature. Still, this formulation is sufficient for the application that does not require high service temperature. Besides, it is postulated that higher peel strength would be obtained if primer or established adhesives were used.

Acknowledgement

References

[1] Hirsch, Jürgen. "Aluminium in innovative light-weight car design." *Materials Transactions* 52, no. 5 (2011): 818-824. https://doi.org/10.2320/matertrans.L-MZ201132

[2] Heide-Jørgensen, Simon, Rasmus Krag Møller, Kristian Birk Buhl, Steen Uttrup Pedersen, Kim Daasbjerg, Mogens Hinge, and Michal K. Budzik. "Efficient bonding of ethylene-propylene-diene M-class rubber to stainless steel using polymer brushes as a nanoscale adhesive." *International Journal of Adhesion and Adhesives* 87 (2018): 31-41. https://doi.org/10.1016/j.ijadhadh.2018.09.006

[3] Souid, Anouar, Alain Sarda, Rémi Deterre, and Eric Leroy. "Rheological characterization and modelling of the rubber to metal vulcanization-bonding process." *Polymer Testing* 36 (2014): 88-94. https://doi.org/10.1016/j.polymertesting.2014.03.020

[4] Mullins, M. J., D. Liu, and H-J. Sue. "Mechanical properties of thermosets." In *Thermosets*, pp. 35-68. Elsevier, 2018. https://doi.org/10.1016/B978-0-08-101021-1.00002-2

[5] Higgins, A. "Adhesive bonding of aircraft structures." *International Journal of Adhesion and Adhesives* 20, no. 5 (2000): 367-376. https://doi.org/10.1016/S0143-7496(00)00006-3

[6] Banea, Mariana D., and Lucas F. M. da Silva. "Adhesively bonded joints in composite materials: an overview." *Proceedings of the Institution of Mechanical Engineers, Part L: Journal of Materials: Design and Applications* 223, no. 1 (2009): 1-18. https://doi.org/10.1243/14644207JMDA219

[7] Hu, P., X. Han, W. D. Li, L. Li, and Q. Shao. "Research on the static strength performance of adhesive single lap joints subjected to extreme temperature environment for automotive industry." *International Journal of Adhesion and Adhesives* 41 (2013): 119-126. https://doi.org/10.1016/j.ijadhadh.2012.10.010

[8] Rahmani, A., and N. Choupani. "Experimental and numerical analysis of fracture parameters of adhesively bonded joints at low temperatures." *Engineering Fracture Mechanics* 207 (2019): 222-236. https://doi.org/10.1016/j.engfracmech.2018.12.031

[9] Poornima, Vijayan P., Debora Puglia, Mariam Ali S. A. Al-Maadeed, Jose M. Kenny, and Sabu Thomas. "Elastomer/thermoplastic modified epoxy nanocomposites: The hybrid effect of 'micro'and 'nano'scale." *Materials Science and Engineering: R: Reports* 116 (2017): 1-29. https://doi.org/10.1016/j.mser.2017.03.001

[10] Pradhan, Sukanya, Priyanka Pandey, Smita Mohanty, and Sanjay Kumar Nayak. "Insight on the chemistry of epoxy and its curing for coating applications: a detailed investigation and future perspectives." *Polymer-Plastics Technology and Engineering* 55, no. 8 (2016): 862-877. https://doi.org/10.1080/03602559.2015.1103269

[11] Wang, Caifeng, Min Zhao, Jun Li, Jiali Yu, Shaofan Sun, Shengsong Ge, Xingkui Guo et al. "Silver nanoparticles/graphene oxide decorated carbon fiber synergistic reinforcement in epoxy-based composites." *Polymer* 131 (2017): 263-271. https://doi.org/10.1016/j.polymer.2017.10.049

[12] Srivastava, V. K. "Effect of carbon nanotubes on the strength of adhesive lap joints of C/C and C/C-SiC ceramic fibre composites." *International Journal of Adhesion and Adhesives* 31, no. 6 (2011): 486-489. https://doi.org/10.1016/j.ijadhadh.2011.03.006

[13] Kinloch, A. J., J. H. Lee, A. C. Taylor, S. Sprenger, C. Eger, and D. Egan. "Toughening structural adhesives via nano- and micro-phase inclusions." *The Journal of Adhesion* 79, no. 8-9 (2003): 867-873. https://doi.org/10.1080/00218460309551

[14] Bhowmik, S., R. Benedictus, J. A. Poulis, H. W. Bonin, and V. T. Bui. "High-performance nanoadhesive bonding of titanium for aerospace and space applications." *International Journal of Adhesion and Adhesives* 29, no. 3 (2009): 259-267. https://doi.org/10.1016/j.ijadhadh.2008.07.002

[15] Sapiai, Napisah, Aidah Jumahat, Mohammad Jawaid, Mohamad Midani, and Anish Khan. "Tensile and flexural properties of silica nanoparticles modified unidirectional kenaf and hybrid glass/kenaf epoxy composites." *Polymers* 12, no. 11 (2020): 2733. https://doi.org/10.3390/polym12112733

[16] Alhazmi, W. H., Yosef Jazaa, S. Mousa, A. A. Abd-Elhady, and H. E. M. Sallam. "Tribological and mechanical properties of epoxy reinforced by hybrid nanoparticles." *Latin American Journal of Solids and Structures* 18 (2021). https://doi.org/10.1590/1679-78256384

[17] Ilyin, Sergey O., and Sergey V. Kotomin. "Effect of Nanoparticles and Their Anisometry on Adhesion and Strength in Hybrid Carbon-Fiber-Reinforced Epoxy Nanocomposites." *Journal of Composites Science* 7, no. 4 (2023): 147. https://doi.org/10.3390/jcs7040147

[18] Rao, Rahul, Cary L. Pint, Ahmad E. Islam, Robert S. Weatherup, Stephan Hofmann, Eric R. Meshot, Fanqi Wu et al. "Carbon nanotubes and related nanomaterials: critical advances and challenges for synthesis toward mainstream commercial applications." *ACS Nano* 12, no. 12 (2018): 11756-11784. https://doi.org/10.1021/acsnano.8b06511

[19] Smith, Andrew T., Anna Marie LaChance, Songshan Zeng, Bin Liu, and Luyi Sun. "Synthesis, properties, and applications of graphene oxide/reduced graphene oxide and their nanocomposites." *Nano Materials Science* 1, no. 1 (2019): 31-47. https://doi.org/10.1016/j.nanoms.2019.02.004

[20] Hung, Pui-yan, Kin-tak Lau, Bronwyn Fox, Nishar Hameed, Joong Hee Lee, and David Hui. "Surface modification of carbon fibre using graphene-related materials for multifunctional composites." *Composites Part B: Engineering* 133 (2018): 240-257. https://doi.org/10.1016/j.compositesb.2017.09.010

[21] Quan, Dong, Declan Carolan, Clemence Rouge, Neal Murphy, and Alojz Ivankovic. "Mechanical and fracture properties of epoxy adhesives modified with graphene nanoplatelets and rubber particles." *International Journal of Adhesion and Adhesives* 81 (2018): 21-29. https://doi.org/10.1016/j.ijadhadh.2017.09.003

[22] Rafiee, Mohammed A., Javad Rafiee, Iti Srivastava, Zhou Wang, Huaihe Song, Zhong-Zhen Yu, and Nikhil Koratkar. "Fracture and fatigue in graphene nanocomposites." *Small* 6, no. 2 (2010): 179-183. https://doi.org/10.1002/smll.200901480

[23] Ahmadi-Moghadam, B., M. Sharafimasooleh, S. Shadlou, and F. Taheri. "Effect of functionalization of graphene nanoplatelets on the mechanical response of graphene/epoxy composites." *Materials & Design* (1980-2015) 66 (2015): 142-149. https://doi.org/10.1016/j.matdes.2014.10.047

[24] Mohamad, N., J. Yaakub, H. E. Ab Maulod, A. R. Jeefferie, M. Y. Yuhazri, K. T. Lau, Q. Ahsan, M. I. Shueb, and R. Othman. "Vibrational damping behaviors of graphene nanoplatelets reinforced NR/EPDM nanocomposites." *Journal of Mechanical Engineering and Sciences* 11, no. 4 (2017): 3274-3287.

[25] Quan, Dong, Neal Murphy, and Alojz Ivankovic. "Fracture behaviour of a rubber nano-modified structural epoxy adhesive: Bond gap effects and fracture damage zone." *International Journal of Adhesion and Adhesives* 77 (2017): 138-150. https://doi.org/10.1016/j.ijadhadh.2017.05.001

[26] Mohamad, N., K. I. Karim, M. Mazliah, H. E. Ab Maulod, J. Abd Razak, M. A. Azam, M. S. Kasim, and R. Izamshah. "Fatigue and mechanical properties of graphene nanoplatelets reinforced NR/EPDM nanocomposites." In *Journal of Physics: Conference Series*, vol. 1082, no. 1, p. 012050. IOP Publishing, 2018. https://doi.org/10.1088/1742-6596/1082/1/012050

[27] Wei, Kam Ka, Teh Pei Leng, Yeoh Cheow Keat, Hakimah Osman, and Lim Bee Ying. "Enhancing compatibility in epoxy/vulcanized natural rubber (VNR)/Graphene nano-platelets (GNP) system using epoxidized natural rubber (ENR-50)." *Composites Part B: Engineering* 174 (2019): 107058. https://doi.org/10.1016/j.compositesb.2019.107058

[28] Ramírez-Herrera, Claudia A., Isidro Cruz-Cruz, Isaac H. Jiménez-Cedeño, Oscar Martínez-Romero, and Alex Elías-Zúñiga. "Influence of the epoxy resin process parameters on the mechanical properties of produced bidirectional [±45°] carbon/epoxy woven composites." *Polymers* 13, no. 8 (2021): 1273. https://doi.org/10.3390/polym13081273

[29] Atieh, Muataz Ali, Omer Yehya Bakather, Bassam Al-Tawbini, Alaadin A. Bukhari, Faraj Ahmad Abuilaiwi, and Mohamed B. Fettouhi. "Effect of carboxylic functional group functionalized on carbon nanotubes surface on the removal of lead from water." *Bioinorganic Chemistry and Applications* 2010 (2010). https://doi.org/10.1155/2010/603978

[30] Du, Jinhong, and Hui-Ming Cheng. "The fabrication, properties, and uses of graphene/polymer composites." *Macromolecular Chemistry and Physics* 213, no. 10-11 (2012): 1060-1077. https://doi.org/10.1002/macp.201200029

[31] Zulkifli, Nor Syazana Adilah, Noraiham Mohamad, ANIS AQILAH ABD GHANI, Siang Yee Chang, Jeefferie Abd Razak, Hairul Effendy Ab Maulod, Mohd Fadli Hassan et al. "Graphene Nanoplatelets Modified Chemlok® Adhesive System

for Natural Rubber-Aluminium Bonded Component in Engine Mount." *International Journal of Automotive and Mechanical Engineering* 19, no. 1 (2022): 9530-9542. https://doi.org/10.15282/ijame.19.1.2022.16.0735

[32] Kim, Ki Hoon, Ji-Un Jang, Gyun Young Yoo, Seong Hun Kim, Myung Jun Oh, and Seong Yun Kim. "Enhanced Electrical and Thermal Conductivities of Polymer Composites with a Segregated Network of Graphene Nanoplatelets." *Materials* 16, no. 15 (2023): 5329. https://doi.org/10.3390/ma16155329

[33] Eakvanich, Visit, Wachara Kalasee, Panya Dangwilailux, Wassachol Wattana, and Juntakan Taweekun. "A Review of the Parameters Related to the Rubber Sheets Production: Major Constituents of Rubber Latex, Rubber Particles, Particle Interaction of Rubber Latex, Rubber Porous Structure, Rubber Drying Kinetics and Energy Consumption." *Journal of Advanced Research in Applied Sciences and Engineering Technology* 29, no. 2 (2023): 159-184. https://doi.org/10.37934/araset.29.2.159184